

# IMAP: Intrinsically Motivated Adversarial Policy

Xiang Zheng  
City University of Hong Kong  
Hong Kong, China  
xzheng235-c@my.cityu.edu.hk

Xingjun ma  
Fudan University  
Shanghai, China  
xingjunma@fudan.edu.cn

Shengjie Wang  
Tsinghua University  
Beijing, China  
shengjiewang@mail.tsinghua.edu.cn

Xinyu Wang  
Tencent  
Shenzhen, China  
xinyucs@gmail.com

Chao Shen  
Xi'an Jiaotong University  
Xi'an, China  
chaoshen@mail.xjtu.edu.cn

Cong Wang  
City University of Hong Kong  
Hong Kong, China  
congwang@cityu.edu.hk

## ABSTRACT

Reinforcement learning (RL) agents are known to be vulnerable to evasion attacks during deployment. In single-agent environments, attackers can inject imperceptible perturbations on the policy or value network's inputs or outputs; in multi-agent environments, attackers can control an adversarial opponent to indirectly influence the victim's observation. Adversarial policies offer a promising solution to craft such attacks. Still, current approaches either require perfect or partial knowledge of the victim policy or suffer from sample inefficiency due to the sparsity of task-related rewards. To overcome these limitations, we propose the Intrinsically Motivated Adversarial Policy (IMAP) for efficient black-box evasion attacks in single- and multi-agent environments without any knowledge of the victim policy. IMAP uses four intrinsic objectives based on state coverage, policy coverage, risk, and policy divergence to encourage exploration and discover stronger attacking skills. We also design a novel Bias-Reduction (BR) method to boost IMAP further. Our experiments demonstrate the effectiveness of these intrinsic objectives and BR in improving adversarial policy learning in the black-box setting against multiple types of victim agents in various single- and multi-agent MuJoCo environments. Notably, our IMAP reduces the performance of the state-of-the-art robust WocaR-PPO agents by 34%-54% and achieves a SOTA attacking success rate of 83.91% in the two-player zero-sum game YouShallNotPass.

## CCS CONCEPTS

• **Computing methodologies** → **Adversarial learning**; Continuous space search; • **Theory of computation** → *Adversarial learning*; • **Computer systems organization** → Robotic control.

## KEYWORDS

adversarial policy, intrinsic motivation, black-box attack

## ACM Reference Format:

Xiang Zheng, Xingjun ma, Shengjie Wang, Xinyu Wang, Chao Shen, and Cong Wang. 2018. IMAP: Intrinsically Motivated Adversarial Policy. In *Proceedings of Make sure to enter the correct conference title from your rights confirmation emai (Conference acronym 'XX)*. ACM, New York, NY, USA, 14 pages. <https://doi.org/XXXXXXX.XXXXXXX>

## 1 INTRODUCTION

Reinforcement Learning (RL) agents are vulnerable to various types of attacks [29, 61], attributed to either the weakness of the function approximators or the inherent weakness of the policies themselves [72]. The growing application of RL agents in safety-critical systems, such as autonomous vehicles [2, 9, 22, 24, 51], healthcare [12, 70], and aerospace [31, 63], highlights the need for developing both certification methods [13, 37, 67, 73] and empirical evaluation methods [16, 33, 50, 58, 73] to verify the robustness of deployed agents. Adversarial policies (AP), as a type of test-time evasion attack, have emerged as a crucial technique for evaluating the robustness of the deployed RL agents [16, 18, 59, 69, 71, 72].

Adversarial policies play an essential role in understanding the vulnerability of RL agents in both single- and multi-agent environments. In single-agent environments, although gradient-based evasion attacks like Fast Gradient Sign Method (FGSM) can craft adversarial perturbations for value or policy networks [33, 49], they have been proven to be suboptimal due to their myopic nature [59]. To find the strongest adversary, Sun [59] proposed Policy Adversarial Actor Director (PA-AD), which involves an adversarial policy trained by RL to find the perturbation direction in the action space of the victim agent and an FGSM-style adversarial actor to craft the corresponding perturbation on the state space of the victim agent. Mo [40] proposed Decoupled Adversarial Policy (DAP) consisting of two sub-policies that select the attacking step and determine the worst-case victim action respectively. However, these white-box methods are unsuitable for attacking deployed RL agents with unknown structures and parameters. To address this, Zhang [72] proposed SA-RL to train a state adversary to directly generate adversarial perturbation on the input of the victim policy. Yu [71] proposed an advRL-GAN framework to generate semantically natural adversarial examples against RL agents with pixel inputs. However, these black-box methods in single-agent environments still require knowledge of the immediate rewards and actions of the victim agent, making it less practical in real scenarios.

Permission to make digital or hard copies of all or part of this work for personal or classroom use is granted without fee provided that copies are not made or distributed for profit or commercial advantage and that copies bear this notice and the full citation on the first page. Copyrights for components of this work owned by others than ACM must be honored. Abstracting with credit is permitted. To copy otherwise, or republish, to post on servers or to redistribute to lists, requires prior specific permission and/or a fee. Request permissions from [permissions@acm.org](mailto:permissions@acm.org).  
*Conference acronym 'XX, June 03–05, 2018, Woodstock, NY*

© 2018 Association for Computing Machinery.  
ACM ISBN 978-1-4503-XXXX-X/18/06...\$15.00  
<https://doi.org/XXXXXXX.XXXXXXX>

Unlike state adversaries that directly disturb the input of the victim policy in single-agent environments, the adversary in multi-agent environments can control an opponent agent to indirectly influence the observation of the victim. Gleave [16] first found this kind of adversarial policy, denoted as AP-MRL. Wu [69] proposed training a surrogate victim model by imitation learning and using an explainable Artificial Intelligent technique to identify the time most critical for the adversarial policy to influence the victim's behavior. Guo [18] developed adversarial policies in non-zero-sum games by simultaneously maximizing the adversary's value function and minimizing the victim's value function. However, existing methods for adversarial policy learning in multi-agent environments are sample-inefficient due to a lack of efficient exploration strategies since task reward functions are usually sparse.

To address the abovementioned issues, we propose Intrinsically Motivated Adversarial Policy (IMAP) to efficiently learn optimal black-box adversarial policy in single- and multi-agent environments without knowledge of the victim policy. We design four intrinsic objectives for IMAP to encourage the adversarial policy to explore novel states. Specifically, the two coverage-driven intrinsic objectives encourage the adversary to maximize the entropy of either the state coverage or the policy coverage, the risk-driven intrinsic objective incites the adversary to minimize the task-agnostic risk function, and the divergence-driven intrinsic objective stimulates the adversary to deviate from its latest policy to force exploration. All intrinsic objectives are designed in the black-box setting without knowledge of the victim policy, including model parameters, immediate rewards, and policy outputs. What's more, we identify that the bias introduced by the intrinsic objectives may distract the adversary in sparse-reward tasks and thus design a bias-reduction method to boost the performance of IAMP further. Our contributions are summarized as follows:

- We propose IMAP, which uses four novel intrinsic objectives (state-coverage-driven, policy-coverage-driven, risk-driven, and divergence-driven) to learn black-box adversarial policies efficiently in both single- and multi-agent environments.
- In single-agent environments, our IMAP outperforms the baseline SA-RL [72] in four dense-reward locomotion tasks when attacking the vanilla PPO and five types of robust RL agents, including two adversarial training methods ATLA [72] and ATLA-SA [72], and three robust regularizer methods SA [73], RADIAL [43], and WocaR [32]. Additionally, it achieves the best results in six sparse-reward locomotion tasks and two sparse-reward navigation tasks compared to SA-RL. We also empirically show that a victim agent that is robust to one type of IMAP might still be vulnerable to another, raising a new challenge for developing robust RL algorithms and stronger evasion attacks.
- In multi-agent environments, our IMAP achieves a SOTA attacking success rate of 83.91% in the two-player zero-sum competitive game YouShallNotPass, outperforming the baseline AP-MRL [16]. The adversary learns a natural blocking skill using the policy-coverage-driven intrinsic objective, shown in Figure 2. In another game KickAndDefend, our IMAP also outperforms AP-MRL.

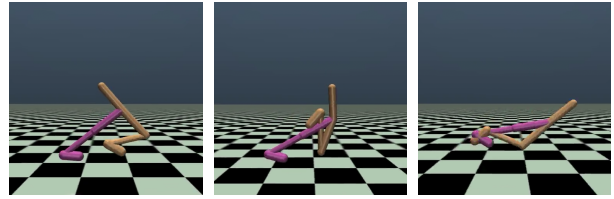


**Figure 1: Visualization of the adversarial behavior learned by IMAP in Walker2d. IMAP can make the state-of-the-art robust model trained by Woca-R-PPO [32] fall down.**

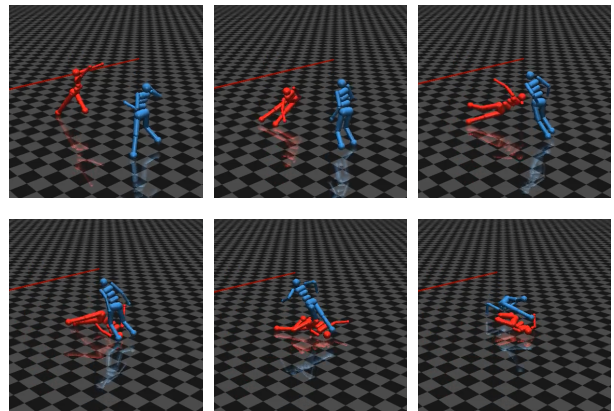


**Figure 2: Visualization of the adversarial behavior learned by IMAP in YouShallNotPass. Instead of sticking in the ground, IMAP encourages the agent to find more effective adversarial behavior like "aggressively" blocking the victim.**

- We develop a novel bias-reduction (BR) method for adversarial policy learning with an approximate extrinsic optimality constraint and empirically demonstrate that BR effectively boosts the performance of IMAP in sparse-reward tasks.

## 2 RELATED WORK

Our work mainly concerns evasion attacks against RL and exploration strategies for sparse-reward RL. In this section, we summarize the state-of-the-art evasion attack and defense methods in the context of RL and intrinsic motivation exploration strategies for sparse-reward RL.

### 2.1 Evasion Attacks Against RL

Existing evasion attacks against RL can be divided into two standard classes: gradient-based adversarial attacks and adversarial policy. Gradient-based adversarial attacks against RL, analogous to FGSM-style adversarial attacks against Deep Neural Network (DNN), craft adversarial examples for the target policy or value networks to deviate the agent from its original trajectories [4, 25, 29, 33, 51, 58]. Adversarial policy instead learns a policy network to generate adversarial perturbations in the state or action space of the victim

agent or determine the timing of the attack in single-agent environments [16, 40, 50, 51, 55, 59, 72], or control an opponent to maliciously create 'natural' observations to attack the victim policy.

**2.1.1 Gradient-Based Evasion Attacks.** Gradient-based evasion attacks are designed to reduce the probability of selecting the optimal action or increase the likelihood of choosing the worst action via FGSM-style attacks. Following the convention of adversarial attacks on DNNs in supervised learning tasks, Lin [33] first investigated adversarial attacks in the context of DRL and showed that existing adversarial example crafting techniques like FGSM could be utilized to significantly degrade the test-time performance of DRL agent in Atari games with pixels-based inputs and discrete actions. Sun [58] promoted the efficiency of such attacks by carefully manipulating the observation of a victim agent at heuristically selected optimal time steps rather than the entire training trajectories. Weng [66] proposed a sample-efficient model-based adversarial attack on DRL agents in continuous control tasks, where the adversary can manipulate either the victim's observations or actions with small perturbations. Lee [29] showed the vulnerability of the DRL agents under the action space adversarial attacks. Zhang [73] proposed two heuristic attacks, Robust Sarsa and Maximal Action Difference, which can be utilized when value functions are unknown.

**2.1.2 Adversarial Policies.** To investigate the robustness of RL agents on state observations under optimal adversarial attack, Zhang introduced an optimal adversary optimized by RL under the SAMDP framework, which was shown to be stronger than existing heuristic evasion attacks [72]. Sun unified the state space and action space perturbations and proposed to first train an adversarial policy to generate the perturbation direction in the low-dimensional action space and then craft the corresponding perturbation in the high-dimensional state space perturbation by gradient-based evasion attacks [59]. Apart from works on optimal adversaries in single-agent environments, adversarial policies are also investigated in multi-agent competition games [15, 16, 18, 65, 69]. Gleave [16] leveraged original Proximal Policy Optimization (PPO) to train the adversarial policy with sparse task rewards and showed that the adversarial policy could successfully induce off-distribution activations in the victim policy network. Wu [69] modified the original PPO loss to encourage the adversary to perturb the critical action of the victim at strategically selected steps. Fujimoto [15] proposed a reward-free adversarial policy by only maximizing the victim policy entropy. Apart from adversarial policies against RL agents in continuous control tasks, Wang [65] recently demonstrated the existence of adversarial policies against the state-of-the-art Go AI system, KataGo.

## 2.2 Defense Against Evasion Attack

Defense methods for RL agents against evasion attack can be mainly divided into four categories: adversarial training [6, 50, 59, 60, 62, 72], robust regularizer [13, 43, 73], randomized smoothing [1, 7, 26, 38, 67], and active detection [19, 34]. Adversarial training has been demonstrated as one of the most popular and empirically successful techniques in robustifying DNN in supervised learning tasks [39]. The adversarial training procedure for RL is similar to the one for DNN, that is, optimizing the policy under attacks via heuristic

gradient-based adversaries or optimal adversarial policies. The adversary in adversarial training can have various access rights to the environment to robustify the victim agent against different types of uncertainties, e.g., directly injecting perturbations to the state or action or reward [6, 59, 60, 62, 68, 72], adding disturbance forces or torques [50], or even changing the layout or dynamic property of the environment [11]. Apart from adversarial training, a regularizer can be applied to robustify the policy. The regularizer can enhance the smoothness of the learned policy by upper-bounding the divergence of the action distributions under state perturbations [57, 73]. Oikarinen [43] proposed a robust deep RL framework with adversarial loss by designing a regularizer to minimize overlap between bounds of actions to avoid choosing a significantly worse action under small state perturbation. Another defense strategy against evasion attack is using randomized smoothing techniques and analyzing the robustness of RL in the probabilistic view [1, 26, 38, 67]. Active detection methods focus on detecting malicious samples by either comparing the KL-divergence of the nominal action distribution and the predicted one [34] or using explainable AI techniques to identify critical time steps contributing to the victim agent's performance [19].

## 2.3 Intrinsic Motivation

Intrinsic motivation is a critical and promising exploration technique for sparse-reward and reward-free RL. It encourages the agent to visit novel states by formulating the agent's familiarity with the environment as the intrinsic objective and measuring the agent's uncertainty as the intrinsic bonus. Intrinsic motivation is mainly developed in two large branches: provable and practical exploration strategies. Provable exploration strategies can guarantee sublinear regret bounds for several Markov Decision Process (MDP) settings like tabular MDP [21, 45] and linear MDP [23, 42, 46, 64]. These provable methods usually utilize the Upper Confidence Bound (UCB) bonus based on *optimism in the face of uncertainty principle* [76] or posterior sampling techniques [44] to balance the exploration and exploit tradeoff. However, it is challenging for these methods to efficiently estimate the UCB bonus or the posterior distribution of the value function. Practical exploration methods instead design approximate intrinsic bonuses to address this challenge. Practical methods are usually classified into three categories: knowledge-based, data-based, and competence-based. Knowledge-based intrinsic motivation methods approximate the novelty via various techniques, including pseudo-count of the state visit frequency [8, 14], prediction errors [10, 47], and variances of outputs of an ensemble of neural networks [3, 28, 48]. Data-based intrinsic motivation is a simple yet promising technique for sparse-reward RL tasks. It formulates the intrinsic objective as state coverage and encourages the agent to cover novel states by maximizing the state entropy [20, 35, 36, 41]. Competence-based methods demand the agent to learn usable and differentiable low-level skills when exploring, which is shown to be too challenging [27, 56].

## 3 PRELIMINARIES

In this section, we introduce the formulations of single- and multi-agent RL tasks and the basic policy gradient method.

### 3.1 Single-Agent RL

In single-agent RL tasks, the target agent interacts with the environment by taking sequential actions according to the observed state at each step, which is usually modeled as an MDP  $M = (\mathcal{S}, \mathcal{A}, P, R_e, \gamma, \mu)$ , where  $\mathcal{S}$  and  $\mathcal{A}$  are the state space and action space,  $P : \mathcal{S} \times \mathcal{A} \rightarrow \Delta(\mathcal{S})$  is a transition function mapping state  $s$  and action  $a$  to the next state distribution  $P(s'|s, a)$ ,  $R_e : \mathcal{S} \times \mathcal{A} \times \mathcal{S} \rightarrow \mathbb{R}$  is the bounded instant extrinsic reward function,  $\gamma \in [0, 1)$  is the discount factor determining the horizon of the process, and  $\mu \in \Delta(\mathcal{S})$  is the initial state distribution. The goal of the target agent is to maximize the expected cumulative rewards.

### 3.2 Multi-Agent RL

For multi-agent RL tasks, we focus on two-player zero-sum competition games. A two-player zero-sum competition game can be formulated as a Markov Game  $M = ((\mathcal{S}_t, \mathcal{S}_o), (\mathcal{A}_t, \mathcal{A}_o), P, (R_e, -R_e), \gamma, \mu)$ , where  $\mathcal{S}_t$  and  $\mathcal{S}_o$  are the state space of the target agent and the opponent agent respectively,  $\mathcal{A}_t$  and  $\mathcal{A}_o$  are the target agent's action space and the opponent agent's action space respectively,  $P : \mathcal{S}_t \times \mathcal{S}_o \times \mathcal{A}_t \times \mathcal{A}_o \rightarrow \Delta(\mathcal{S}_t, \mathcal{S}_o)$  is the transition function where  $\Delta(\mathcal{S}_t, \mathcal{S}_o)$  is the space of the probability distribution over both  $\mathcal{S}_t$  and  $\mathcal{S}_o$ ,  $R_e : \mathcal{S}_t \times \mathcal{S}_o \times \mathcal{A}_t \times \mathcal{A}_o \times \mathcal{S}_t \times \mathcal{S}_o \rightarrow \mathbb{R}$  is the bounded instant extrinsic reward function for the target agent,  $-R_e$  is the extrinsic reward function for the opponent agent according to the zero-sum assumption,  $\gamma \in [0, 1)$  is the common discount factor determining the horizon of the game, and  $\mu \in \Delta(\mathcal{S})$  is the initial state distribution. When one agent's policy is fixed, the state transition of the Markov Game will depend only on the other agent's policy instead of the joint policy.

### 3.3 Policy Optimization

As stated in Section 3.1, the target agent tries to maximize the expected total rewards. For a policy  $\pi$ , we can use the value function  $V^\pi : \mathcal{S} \rightarrow \mathbb{R}$  to represent the discounted sum of future intrinsic rewards starting from the state  $s$

$$V^\pi(s) = \mathbb{E}_{\tau \sim P(\cdot|\mu, \pi)} [R(\tau)|s_0 = s], \quad (1)$$

where  $\tau = (s_0, a_0, s_1, a_1, \dots)$  is the trajectory,  $P(\tau|\mu, \pi)$  is the distribution of  $\tau$  induced by the policy  $\pi$  with the initial state distribution  $\mu$ ,

$$P(\tau|\mu, \pi) = \mu(s_0) \prod_{t=0}^{\infty} P(s_{t+1}|s_t, a_t) \pi(a_t|s_t), \quad (2)$$

and  $R(\tau)$  is the discounted cumulative extrinsic reward along a trajectory  $\tau$

$$R(\tau) = \sum_{t=0}^{\infty} \gamma^t r_t^e, \quad (3)$$

where  $r_t^e := R_e(s_t, a_t, s_{t+1})$  is the extrinsic reward function. Similarly, the action-value function  $Q^\pi : \mathcal{S} \times \mathcal{A} \rightarrow \mathbb{R}$  is defined as

$$Q^\pi(s, a) = \mathbb{E}_{\tau \sim P(\cdot|\mu, \pi)} [R(\tau)|s_0 = s, a_0 = a] \quad (4)$$

The goal of the agent is to find a policy  $\pi_\theta$  that maximizes the value, and the optimization problem can be represented as

$$\max_{\theta} V^{\pi_\theta}(\mu). \quad (5)$$

where  $V^{\pi_\theta}(\mu) := \mathbb{E}_{s \sim \mu} V^{\pi_\theta}(s)$ . According to the performance difference lemma, we can rewrite  $V^{\pi_\theta}(\mu)$  as

$$V^{\pi_\theta}(\mu) = V^{(k)}(\mu) + \mathbb{E}_{s \sim d^{\pi_\theta}, a \sim \pi_\theta} \left[ \frac{1}{1-\gamma} A^{(k)}(s, a) \right], \quad (6)$$

where  $d^{\pi_\theta}(s) := (1-\gamma) \sum_{t=0}^{\infty} \gamma^t P(s_t = s | \mu, \pi_\theta)$  is the state distribution induced by  $\pi_\theta$  with the initial state distribution  $\mu$ ,  $V^{(k)} := V^{\pi_{\theta_k}}$  is the value function at the  $k$ -th iteration,  $A^{(k)}(s, a) := Q^{\pi_{\theta_k}}(s, a) - V^{(k)}(s)$  is the advantage function. Note that according to the definition of  $d_\mu^{\pi_\theta}$ , Equation (5) can also be represented as

$$\max_{d^\pi} J_e(d^\pi), \quad (7)$$

where  $J_e(d^\pi) := \sum_s d^\pi(s) \hat{r}^e(s)$  is also called the extrinsic objective,  $\hat{r}^e(s) = \mathbb{E}_{a \sim \pi, s' \sim P} R_e(s, a, s')$  is the instant extrinsic reward at state  $s$ .

Trust-Region Policy Optimization (TRPO) introduced by Schulman [52] guarantees monotonic improvement of the policy by constraining the KL-divergence between the new policy and the old policy as following

$$\begin{aligned} \max_{\theta} \mathbb{E}_{s \sim d_\mu^{(k)}, a \sim \pi_\theta} [A^{(k)}(s, a)] \\ \text{s.t. } D_{\text{KL}}(\text{Pr}_\mu^{(k)} \parallel \text{Pr}_\mu^{\pi_\theta}) \leq \delta, \end{aligned} \quad (8)$$

where  $d_\mu^{(k)} := d_\mu^{\pi_{\theta_k}}$  is the state visitation induced by  $\pi_{\theta_k}$  with the initial state distribution  $\mu$ ,  $\text{Pr}_\mu^{(k)} := \text{Pr}_\mu^{\pi_{\theta_k}}$  is the trajectory distribution induced by the policy  $\pi_{\theta_k}$ ,  $D_{\text{KL}}(P_1 \parallel P_2)$  is the KL-divergence between two distributions  $P_1$  and  $P_2$ .

Proximal Policy Optimization (PPO) [54] avoids complex second-order optimization involved in Equation (8) by constructing a new objective function to minimize

$$\begin{aligned} L_k^{\text{PPO}}(\theta) = \mathbb{E}_{s_t \sim d_\mu^{(k)}, a_t \sim \pi_{\theta_k}} \min \left\{ \frac{\pi_\theta(a_t|s_t)}{\pi_{\theta_k}(a_t|s_t)} \hat{A}_t, \right. \\ \left. \text{clip} \left( \frac{\pi_\theta(a_t|s_t)}{\pi_{\theta_k}(a_t|s_t)}; 1-\epsilon, 1+\epsilon \right) \hat{A}_t \right\}, \end{aligned} \quad (9)$$

where

$$\text{clip}(x; 1-\epsilon, 1+\epsilon) = \begin{cases} 1-\epsilon, & x \leq 1-\epsilon \\ 1+\epsilon, & x \geq 1+\epsilon \\ x, & \text{otherwise} \end{cases} \quad (10)$$

is the clipping function,

$$\hat{A}_t = \sum_{l=0}^{\infty} (\gamma \lambda)^l (r_{t+l}^e + \gamma V^{(k)}(s_{t+l+1}) - V^{(k)}(s_{t+l})) \quad (11)$$

is the Generalized Advantage Estimation (GAE) [53]. The clipping function makes sure that the policy gradient is zero when  $r^{(k)} \notin [1-\epsilon, 1+\epsilon]$ ; GAE is able to reduce the variance of policy gradient estimates; the outer minimization operator ensures the objective function  $L_k^{\text{PPO}}(\theta)$  is a lower bound of the original objective. PPO then utilizes multiple steps of mini-batch stochastic gradient ascent on  $L_k^{\text{PPO}}(\theta)$  with a dataset  $\mathcal{D} := \{(s_t, a_t, r_t^e, s_{t+1})\}_{t=0}^N$  collected by the old stochastic policy  $\pi_{\theta_k}$ .

## 4 THREAT MODEL

In this section, we define the threat model for black-box adversarial policy learning in single- and multi-agent RL tasks.

### 4.1 Threat Model for Single-Agent RL

In single-agent RL tasks, the goal of the evasion attacker is to reduce the expected cumulated extrinsic reward of the target agent  $V^{\pi^v}(\mu)$ , where  $\pi^v$  is the policy of the target (victim) agent parameterized by fixed deterministic parameters. Note that when the extrinsic reward signal is the indicator of task completion,  $V^{\pi^v}(\mu)$  is equal to the success rate of the task under the policy  $\pi^v$ . The attacker does not know  $\pi^v$ , including the target policy network’s architecture, hyperparameters, parameters, activations, and outputs. The attacker also has no knowledge of the environment dynamics or permission to change the environment directly. What’s more, the attacker is assumed to be unaware of the shaping or intrinsic reward function utilized by the victim agent for training  $\pi^v$  before deployment. This assumption is reasonable since the reward signal and the corresponding value network in the training phase are usually unnecessary for using  $\pi^v$  in the deployment phase. Thus, the adversary can only leverage the sparse extrinsic signal to determine whether the evasion attack is successful. The adversary only has the right to access the input  $s$  of the victim policy  $\pi^v$  and is restricted to adding small bounded perturbations to  $s$  to make the attack imperceptible. The adversary can query the victim model, e.g., collecting the rollouts of the victim policy. Formally, we model the state adversary as  $a^a \sim \pi^a(\cdot|s)$ , which generates an adversarial perturbation  $a^a$  based on the victim’s current state. The perturbation  $a^a$  is usually bounded in an  $\ell_p$  norm ball with a constant small radius  $\epsilon$ , that is,  $\|a^a\|_p \leq \epsilon$  [72]. The transition functions for the adversary and the victim under this threat model becomes

$$P^a(s_{t+1}|s_t, a_t^a) = P(s_{t+1}|s_t, \pi_v(s_t + a_t^a)). \quad (12)$$

### 4.2 Threat Model for Multi-Agent RL

As stated in Section 3.2, we focus on two-player zero-sum competition games in this paper where the sum of the two agents’ rewards equals zero for any state transition. We assume that the evasion attacker can control the opponent agent of the target agent to indirectly degrade the victim’s performance. Similar to the single-agent black-box evasion attack, the adversary’s goal is to minimize the expected cumulative extrinsic reward of the victim. The adversary is also ignorant of the victim’s policy model, including the network structure, parameters, activations, and output. The target agent follows a fixed deterministic policy  $\pi_v$ , in accordance with the common case where the parameters of the deployed safety-critical policy network are usually static or infrequently updated. When the victim policy is held fixed, the two-player Markov game  $M$  reduces to a single-player MDP  $M^a = ((S_v, S_a), \mathcal{A}_a, P_a, R_a)$  for the evasion attacker to solve, where  $P^a : S_v \times S_a \times \mathcal{A}_a \rightarrow \Delta(S_v, S_a)$  is the transition function with the fixed victim policy  $\pi_v$  embedded [18]. In each interaction step, the victim agent takes its action  $a_t^v = \pi^v(s_t^v, s_t^a)$  according to the fixed deterministic policy and current state, while the adversary samples its action from the stochastic policy  $a_t^a \sim \pi^a(s_t^v, s_t^a)$ . The transition function for the adversary

under this threat model is then

$$P^a(s_{t+1}^v, s_{t+1}^a | s_t^v, s_t^a, a_t^a) = P(s_{t+1}^v, s_{t+1}^a | s_t^v, a_t^v, a_t^a). \quad (13)$$

## 5 INTRINSIC OBJECTIVES FOR IMAP

In this section, we design appropriate intrinsic objectives for black-box adversarial policy learning. According to our threat models, the adversary cannot fetch either the target agent policy’s gradient or output. Thus, it cannot craft adversarial examples for the target policy via FGSM or train a surrogate target model to utilize the transferability of adversarial examples. Moreover, the adversary does not know the value network and the reward function utilized by the target agent in the training phase, making it even more challenging for the adversary to solve. To facilitate adversarial policy learning in the black-box setting, we leverage intrinsic motivation to encourage the adversary to discover novel attacking strategies. Intrinsic motivation is a promising exploration technique for sparse-reward RL. Formally, we use the following general objective function for black-box adversarial policy learning with intrinsic objective as a regularizer:

$$L_k(d^{\pi^a}) = J_e^a(d^{\pi^a}) + \tau_k J_i(d^{\pi^a}; \{d^{\pi_i^a}\}_{i=1}^k), \quad (14)$$

where  $J_e^a(d^{\pi^a}) := -\sum_s d^{\pi^a}(s) \hat{r}^e(s)$  is the extrinsic objective of the adversary,  $r^e$  is the victim agent’s extrinsic reward,  $J_i(d^{\pi^a}; \{d^{\pi_i^a}\}_{i=1}^k)$  is the intrinsic objective which is a function of the state distribution induced by the adversarial policy  $\pi^a$  and state distributions induced by all prior adversarial policies  $\pi_1^a, \dots, \pi_k^a$ .  $\tau_k$  is the temperature parameter determining the strength of the regularizer. Note here we use a surrogate extrinsic reward function  $\hat{r}^e(s)$  instead of the true extrinsic reward function  $r^e(s)$  utilized by the victim agent since the adversary is assumed to be unaware of  $r^e(s)$  and has to design a surrogate extrinsic reward function according to the task type. We further discuss the choice of the surrogate extrinsic reward function in Section 6.1.

We design four appropriate intrinsic objectives  $J^i(d^{\pi^a})$  for black-box adversarial policy learning to encourage the adversary to explore novel states, including two coverage-driven intrinsic objectives, one diversity-driven objective, and one risk-driven intrinsic objective. We first introduce the state-coverage-driven intrinsic objective, which encourages the adversary to lure the victim agent into covering a specific induced state distribution. We then present a policy-coverage-driven intrinsic objective to incite the adversary to maximize the deviation of the occupancy of the victim policy from its optimal trajectories. Inspired by constrained reinforcement learning, we also propose a risk-driven intrinsic objective by designing a heuristic task-agnostic risk function for the adversary to restrict the victim’s dynamic behavior, expected to reduce the performance of the victim policy. Last, diversity-driven exploration stimulates the adversary to keep deviating the new adversarial policy from the old ones by maximizing their KL-divergence. Though these intrinsic objectives can encourage the adversary to explore novel states, the adversary might be distracted by the introduced intrinsic objectives in sparse-reward tasks. To decrease the bias introduced by these intrinsic objectives, we also propose an approximate extrinsic optimality constraint for Equation (14) to ensure the adversarial policy is approximately optimal with respect to the

expected extrinsic reward and discuss the choice of the temperature parameter  $\tau_k$ .

## 5.1 Coverage-Driven Intrinsic Objective

Current adversarial policy learning in single- and multi-agent RL tasks uses heuristic dithering exploration methods that randomly perturb the optimal actions regardless of the agent's learning process, which has been shown to be inefficient when the extrinsic reward is sparse. To address this issue, we introduce two coverage-driven intrinsic objectives for black-box sparse-reward adversarial policy learning. Note the design of the intrinsic objectives for the adversary can be slightly different in single- and multi-agent RL tasks due to differences in their MDP modeling.

**5.1.1 State Coverage for Single-Agent RL.** State coverage (SC) is a natural choice to be the intrinsic objective when the extrinsic reward is sparse, which is also known as state distribution matching. SC encourages the adversary to lure the victim into covering a certain state distribution, analogous to targeted evasion attacks in image classification tasks. Since we focus on untargeted evasion attacks, we choose uniform distribution  $\mathcal{U}$  as a natural target distribution, that is,

$$J_i^{\text{SC}}(d^{\pi^a}) = -D_{\text{KL}}(d^{\pi^a} \parallel \mathcal{U}), \quad (15)$$

which is equivalent to the state entropy

$$J_i^{\text{SC}}(d^{\pi^a}) = - \sum_s d^{\pi^a}(s) \ln d^{\pi^a}(s). \quad (16)$$

By maximizing  $J_i^{\text{SC}}$ , the adversary lures the victim agent to cover the state space as uniformly as possible. For a non-robust victim policy, recovering from an unseen state to the optimal trajectory will be hard.

**5.1.2 State Coverage for Multi-Agent RL.** For multi-agent RL tasks, the adversary can not only lure the victim into covering a certain state distribution but also enforce itself to match a certain state distribution. When some prior knowledge exists, the adversary can leverage the prior to facilitate the learning process, similar to imitation learning. When there is no prior available, the adversary can choose to maximize its own state entropy to visit novel states more efficiently when the extrinsic reward is sparse. We first define marginal state distribution as

$$d_{\mathcal{Z}}^{\pi}(z) = (1 - \gamma) \sum_{t=0}^{\infty} \gamma^t P(\Pi_{\mathcal{Z}} s_t = z | \mu, \pi_{\theta}), \quad (17)$$

where  $\Pi_{\mathcal{Z}}$  is an operator mapping the full state into a low-dimensional projection space  $\mathcal{Z}$ ,  $\mathcal{Z}$  can represent a subspace of  $\mathcal{S}$ , or a latent space generated by dimension reduction methods like Principle Component Analysis (PCA) or an Autoencoder. The SC-driven intrinsic objective for black-box adversarial policy learning in multi-agent RL tasks is then formulated as following

$$J_i^{\text{SC-M}}(d^{\pi^a}) = (1 - \alpha^v) J_i^{\text{SC}}(d_{\mathcal{S}_a}^{\pi^a}) + \alpha^v J_i^{\text{SC}}(d_{\mathcal{S}_v}^{\pi^a}), \quad (18)$$

where  $\alpha^v$  is a balancing constant for the two sub-objectives.

**5.1.3 Policy Coverage for Single-Agent RL.** Instead of luring the victim policy to a target state distribution, policy coverage (PC) aims to encourage the adversary to derail the victim policy from the optimal trajectories by maximizing the deviation of the state distribution  $d^{\pi}$  induced by the next perturbed victim policy from the policy coverage  $\rho^k$  induced by all prior policies. Policy coverage  $\rho^k$  is defined as a uniform combination of past visitation densities [74], that is,  $\rho^k = \sum_{i=1}^k d^{\pi_i^a}$ . Similar to SC, we define the PC-driven intrinsic objective as the entropy of the policy coverage  $\rho^k$ , that is,

$$J_i^{\text{PC}}(d^{\pi^a}) = - \sum_s \rho^k(s) \ln \rho^k(s). \quad (19)$$

By maximizing the entropy of the policy coverage, the victim policy will be gradually lured to be away from its optimal trajectories.

**5.1.4 Policy Coverage for Multi-Agent RL.** Similar to the design of the state-coverage-based intrinsic objective for black-box adversarial policy learning in single-agent tasks, we propose a policy-coverage-based intrinsic objective for multi-agent scenarios as

$$J_i^{\text{PC-M}}(d^{\pi^a}) = (1 - \alpha^v) J_i^{\text{PC}}(d_{\mathcal{S}_a}^{\pi^a}) + \alpha^v J_i^{\text{PC}}(d_{\mathcal{S}_v}^{\pi^a}), \quad (20)$$

where  $\rho_{\mathcal{S}}^k := \sum_{i=1}^k d_{\mathcal{S}}^{\pi_i^a}$  is the marginal policy cover. The first term encourages the adversary to control the opponent agent to cover more states instead of struggling in place. The second term rewards the adversary for inducing the victim to cover novel states to exploit the victim policy's potential weakness.

**5.1.5 State Density Approximation.** Since all the coverage-based intrinsic objectives involve state density, selecting appropriate state density approximation methods is crucial. In current related works, there are two main types of methods to approximate state density, i.e., prediction-error-based estimation and  $\kappa$ -nearest-neighbour ( $\kappa$ -NN) estimation. Prediction-error-based estimation like ICM [47] or RND [10] utilizes the prediction error of a neural network at a specific state  $s$  to represent its sparsity (inverse of state density). However, it may suffer from forgetting problems [74, 75]. We thus turn to  $\kappa$ -NN estimation, which is more efficient and stable [36, 77].

*$\kappa$ -NN estimation.*  $\kappa$ -NN estimation is a nonparametric estimation method. It expresses the sparsity of a state via the distance between the state and its  $k$ -nearest neighbor, that is,

$$\hat{\rho}^k(s) = \frac{1}{\|s - s_{\mathcal{B}}^k\|}, \quad (21)$$

where  $s_{\mathcal{B}}^k \in \mathcal{B}$  is the  $\kappa$ -nearest state of state  $s$  in the replay buffer  $\mathcal{B}$ . Note that  $\mathcal{B}$  includes all history trajectories sampled by  $\pi_1^a, \dots, \pi_k^a$ . A more stable version of  $k$ -NN estimation is

$$\hat{\rho}^k(s) = \frac{\kappa}{\sum_{j=1}^{\kappa} \|s - s_{\mathcal{B}}^j\|}, \quad (22)$$

which uses the average distance instead of the maximum distance. For the state density  $d^{\pi^a}$ , since we cannot use the next policy  $\pi^a$  to directly sample trajectories, we can approximate it using the trajectories sampled by the latest policy  $\pi_k^a$  under the assumption that the two policies are similar, that is,

$$\hat{d}^{\pi^a}(s) = \frac{\kappa}{\sum_{j=1}^{\kappa} \|s - s_{\mathcal{D}}^j\|}, \quad (23)$$

where  $\mathcal{D}$  is a replay buffer containing only trajectories sampled by the latest policy  $\pi_k^a$ .

## 5.2 Risk-Driven Intrinsic Objective

Apart from the coverage-driven intrinsic objective, we also propose a novel risk-driven intrinsic objective for black-box adversarial policy learning. Inspired by the constrained RL where a cost function is defined to penalize the agent’s inappropriate behavior, we design a heuristic intrinsic objective for the adversary based on a task-agnostic risk function, that is,

$$J_i^R(d^{\pi^a}) = - \sum_s d^{\pi^a}(s) \|s - s_0\|. \quad (24)$$

where  $s_0 \sim \mu$  is the initial state of the agent. Intuitively, this risk-based intrinsic objective encourages the adversary to make the target agent stuck near the initial state instead of following the optimal trajectories. It differs from reward shaping since it is task-agnostic with no need for task-domain knowledge. Though it is simple, we show its effectiveness in certain tasks, especially those with termination mechanisms, that is, the episode will be terminated when the agent steps into dangerous states predefined by the environment. For multi-agent tasks, we can define a similar risk-driven intrinsic objective as

$$J_i^{R-M}(d^{\pi^a}) = - \sum_s d_{S_v}^{\pi^a} \|\Pi_{S_v} s - \Pi_{S_v} s_0\|. \quad (25)$$

Here we use the projected state of the victim agent to calculate the risk instead of the joint state since we only expect the victim agent to be stuck near the initial state.

## 5.3 Diversity-Driven Intrinsic Objective

The diversity-driven intrinsic objective encourages the adversary to explore different behaviors by continuously enforcing the next adversarial policy deviating from its prior ones. This way, the adversary is expected to explore novel attacking strategies instead of falling into local optimality. To achieve this goal, we first introduce a mimic policy  $\pi^m$  to learn the behavior of the adversarial policy. The mimic policy is updated by solving the following optimization,

$$\min_{\pi^m} \sum_s d^{\pi_k^a}(s) D_{\text{KL}}(\pi_k^a(s), \pi^m(s)), \quad (26)$$

that is, minimizing the KL divergence between the latest policy  $\pi_k^a$  and the mimic  $\pi^m$ . Equation (26) can be solved by Stochastic Gradient Descent (SGD). Under the assumption that the next policy  $\pi^a$  is similar to the latest policy  $\pi_k^a$ , we then design the diversity-driven intrinsic objective for black-box adversarial policy as follows

$$J_i^D(d^{\pi^a}) = \sum_s d^{\pi^a}(s) D_{\text{KL}}(\pi_k^a(s), \pi_k^m(s)). \quad (27)$$

Note that  $D_{\text{KL}}(\pi_k^a(s), \pi_k^m(s))$  does not depend on  $d^{\pi^a}$  and Equation (27) is thus a linear function of  $d^{\pi^a}$ . The objective  $J_i^D$  encourages the adversary to visit states where the KL divergence between the latest adversarial policy and the mimic policy is large. In practice, we usually select a smaller learning rate for the mimic to stabilize the learning. Intuitively, the delayed update for the mimic prevents the adversary from having to constantly adapt.

## 5.4 Solving the Regularized Objective

We now present how to maximize the regularized objective  $L^k(d^{\pi^a})$  defined in Equation (14). It is easy to verify that  $L^k(d^{\pi^a})$  is a concave function of  $d^{\pi^a}$  when using any previously defined intrinsic objective. We leverage the Frank-Wolfe algorithm (also known as the conditional gradient method) to solve  $\max_{d^{\pi^a}} L^k(d^{\pi^a})$ . Frank-Wolfe algorithm iteratively solves the following problem

$$d^{\pi_{k+1}^a} \in \arg \max_d \left\langle d, \nabla_{d^{\pi^a}} L_k(d^{\pi^a}) \Big|_{d^{\pi^a} = d^{\pi_k^a}} \right\rangle \quad (28)$$

to construct a sequence of estimates  $d^{\pi_0^a}, d^{\pi_1^a}, \dots$  that converges to a solution of the regularized objective. The R.H.S. is also known as the Frank-Wolfe gap. Note that maximizing the Frank-Wolfe gap is equivalent to finding a policy  $\pi_{k+1}^a$  that maximizes the expected cumulative rewards, which is in proportion to the derivative of  $L^k(d^{\pi^a})$ . We thus define the intrinsic bonus as

$$r_k^i = \nabla_{d^{\pi^a}} L_k(d^{\pi^a}) \Big|_{d^{\pi^a} = d^{\pi_k^a}} \quad (29)$$

We propose a modified PPO objective based on the intrinsic bonus as

$$L_k^{\text{PPO}}(\theta) = \mathbb{E}_{s_t \sim d_{\mu}^{(k)}, a_t \sim \pi_{\theta_k}} \min \left\{ \frac{\pi_{\theta}(a_t | s_t)}{\pi_{\theta_k}(a_t | s_t)} \tilde{A}_t, \text{clip} \left( \frac{\pi_{\theta}(a_t | s_t)}{\pi_{\theta_k}(a_t | s_t)}; 1 - \epsilon, 1 + \epsilon \right) \tilde{A}_t \right\}, \quad (30)$$

where

$$\begin{aligned} \tilde{A}_t &= \hat{A}_t + \tau_k \hat{A}_t^i \\ \hat{A}_t^i &= \sum_{l=0}^{\infty} (\gamma \lambda)^l (r_{t+l}^i + \gamma V_i^{(k)}(s_{t+l+1}) - V_i^{(k)}(s_{t+l})). \end{aligned} \quad (31)$$

We use  $\tilde{A}_t$  to denote the weighted advantage function.  $V_i^{(k)}(s) = \mathbb{E} [\sum_{t=0}^{\infty} \gamma^t r_t^i | s_0 = s]$  is the intrinsic value function under the policy  $\pi_k^a$ .  $V_i^{(k)}$  is usually approximated by a neural network with parameters  $\phi_k^i$  and denoted as  $V_{\phi_k^i}$ .  $\hat{A}_t^i$  is the GAE calculated with intrinsic rewards and intrinsic value functions. The extrinsic value function  $V_{\phi^e}$  and the intrinsic value function  $V_{\phi^i}$  is updated by solving the following regressions via SGD

$$\begin{aligned} \phi_{k+1}^e &= \arg \min_{\phi^e} \mathbb{E}_{s_t \sim d_{\mu}^{(k)}} \|V_{\phi^e}(s_t) - (V_{\phi_k^e}(s_t) + \hat{A}_t)\|, \\ \phi_{k+1}^i &= \arg \min_{\phi^i} \mathbb{E}_{s_t \sim d_{\mu}^{(k)}} \|V_{\phi^i}(s_t) - (V_{\phi_k^i}(s_t) + \hat{A}_t^i)\|. \end{aligned} \quad (32)$$

Algorithm 1 shows the total solution for intrinsically motivated black-box adversarial policy learning.

## 5.5 Reducing Bias of Intrinsic Objective

The regulator in Equation (14) may introduce bias, that is, the policy which maximizes the regularized objective  $L_k(d^{\pi^a})$  cannot be guaranteed to maximize the extrinsic objective  $J_e^a(d^{\pi^a})$ . A common practice to reduce the bias is to carry out a sufficient hyperparameter search to find the best sequences of the temperature parameter  $\lambda_1, \dots, \lambda_k$  for different tasks. A more adaptive way is to introduce an extrinsic optimality constraint to prevent the agent from being

**Algorithm 1** IMAP

---

Initialize the adversarial policy  $\pi_\theta^a$  and its value functions  $V_{\phi^e}$  and  $V_{\phi^i}$   
Initialize replay buffers  $\mathcal{B}$  and  $\mathcal{D}$   
Initialize the Lagrangian multiplier  $\lambda_0 = 0$ , the step counter  $t = 0$ , and the batch counter  $k = 0$   
**while**  $t < T$  **do**  
  Collect samples  $\mathcal{D} = \{(s_t, a_t, r_t^e, s_{t+1})\}$  using  $\pi_{\theta_k}^a$   
  Update replay buffer  $\mathcal{B} = \mathcal{B} \cup \mathcal{D}$   
   $t = t + \text{len}(\mathcal{D})$   
  compute intrinsic rewards  $r_k^i$  via Equation (29)  
  Compute advantage  $\tilde{A}^t$  via Equation (31)  
  Update  $\theta$  via Equation (30)  
  Update  $\phi^e$  and  $\phi^i$  via Equation (32)  
  Update  $\lambda_k$  via Equation (37)  
   $k = k + 1$   
**end while**

---

distracted from the intrinsic rewards. The constrained optimization problem for black-box adversarial policy learning is

$$\begin{aligned} \max_{d^{\pi^a}} J_e^a(d^{\pi^a}) + J_i(d^{\pi^a}) \\ \text{s.t. } J_e^a(d^{\pi^a}) = \max_d J_e^a(d). \end{aligned} \quad (33)$$

It can be viewed to first find a policy  $d^{\pi^a}$  that maximizes  $L_k(d^{\pi^a})$ , and then check whether this policy satisfies the constraint. Apparently,  $\max_{d^{\pi^a}} J_e^a(d^{\pi^a}) = 1$  when the extrinsic reward signal is the task success indicator, which makes the constraint too hash. To solve Equation (46) efficiently without introducing complex optimization mechanisms, we propose approximate extrinsic optimality constraint as a soft adaptive constraint

$$\begin{aligned} \max_{d^{\pi^a}} J_e^a(d^{\pi^a}) + J_i(d^{\pi^a}) \\ \text{s.t. } J_e^a(d^{\pi^a}) \geq \beta J_e^a(d^{\pi_{k-1}^a}), \end{aligned} \quad (34)$$

where the hyperparameter  $\beta \geq 1$  is to adjust the constraint strength. Instead of training another policy to evaluate  $J_e^a(d^{\pi^a})$ , we assume that the performance of the policy  $d^{\pi_{k-1}^a}$  that maximizes  $L_{k-1}(d^{\pi^a})$  is similar to the policy that maximizes  $J_e^a(d^{\pi^a})$  at  $k$  iteration.

To solve the soft-constrained optimization problem, we leverage the Lagrangian method to convert it into an unconstrained min-max optimization problem. Define  $b_{k-1} := \beta J_e^a(d^{\pi_{k-1}^a})$ , the Lagrangian of Equation (34) is then

$$\begin{aligned} \mathcal{L}(d^{\pi^a}, \lambda) = & J_e^a(d^{\pi^a}) + J_i(d^{\pi^a}) \\ & + \lambda(J_e^a(d^{\pi^a}) - b_{k-1}) \\ = & (1 + \lambda)J_e^a(d^{\pi^a}) + J_i(d^{\pi^a}) - \lambda b_{k-1}, \end{aligned} \quad (35)$$

where  $\lambda$  is the Lagrangian multiplier. The corresponding dual problem is

$$\min_{\lambda \geq 0} \max_{d^{\pi^a}} \mathcal{L}(d^{\pi^a}, \lambda). \quad (36)$$

The Lagrangian multiplier  $\lambda$  can be updated by stochastic gradient descent

$$\lambda_k = \lambda_{k-1} - \eta(J_e^a(d^{\pi_k^a}) - b_{k-1}), \quad (37)$$

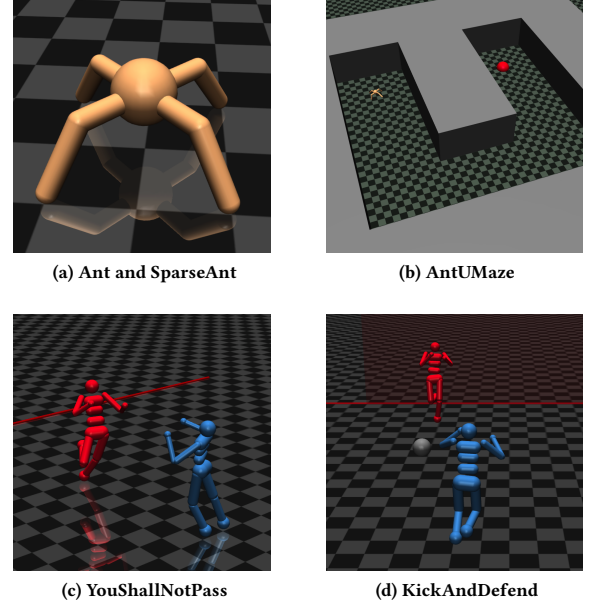


**Figure 3: Rendered pictures of typical MuJoCo environments we used to evaluate IMAP. ?? the dense-reward single-agent locomotion task Ant and the sparse-reward single-agent locomotion task SparseAnt; ?? the sparse-reward single-agent navigation task AntUMaze; ?? & ?? two sparse-reward multi-agent competition tasks YouShallNotPass and KickAndDefend where the blue human is controlled by the victim policy and the red human is controlled by the adversarial policy.**

where  $\eta$  is the updating step size. The Lagrangian implies an interpretation for  $\lambda$ , that is, when  $\lambda$  increases, it encourages the agent to pay more attention to the extrinsic objective. To make the learning process more stable, we use the following "normalized" bias-reduction (BR) objective

$$\begin{aligned} \hat{\mathcal{L}}(d^{\pi^a}, \lambda_{k-1}) = & \frac{1}{1 + \lambda_{k-1}} (\mathcal{L}(d^{\pi^a}, \lambda_{k-1}) + \lambda b_{k-1}) \\ = & J_e^a(d^{\pi^a}) + \tau_k J_i(d^{\pi^a}), \end{aligned} \quad (38)$$

where

$$\tau_k = \frac{1}{1 + \lambda_{k-1}} \quad (39)$$

is the temperature parameter.

## 6 EXPERIMENTS

In this section, we conduct comprehensive experiments in various types of single- and multi-agent RL tasks to evaluate the attack capacity of our IMAP equipped with four different intrinsic objectives.



## 6.1 Experiment Setup

We evaluate our CIM on both single-agent and multi-agent RL tasks. All environments are implemented based on the OpenAI Gym library. In single-agent environments, we select 1) four dense-reward locomotion tasks, including Hopper, Walker2d, HalfCheetah, and Ant; 2) six sparse-reward locomotion tasks, including SparseHopper, SparseWalker2d, SparseHalfCheetah, SparseAnt, SparseHumanoidStandup, and SparseHumanoid; 3) one sparse-reward navigation task, AntUMaze. We select two two-player zero-sum competition games for multi-agent RL tasks, including YouShallNotPass and KickAndDefend.

### 6.1.1 Dense-Reward Single-Agent Locomotion Tasks.

*Task Description.* In the four dense-reward locomotion tasks, the victim agent is expected to run as fast as possible and live as long as possible. The maximum length of one episode is set to be 1000 timesteps. The victim agent is trained to maximize the average episode cumulative rewards. The dense instant extrinsic reward function in these tasks is defined as follows

$$r^{e1} = v_x - \omega_a \|a\|^2 - \omega_f \|f\|^2 + b_1, \quad (40)$$

where  $v_x$  is the forward velocity of the robot,  $a$  is the action vector output by the target policy,  $f$  is the contact force vector clipped from -1 to 1 elementwise,  $\omega_a$  and  $\omega_f$  are two task-dependent constant coefficients, and  $b$  is the constant living bonus. According to the threat model defined in Section 4, the adversary is assumed to have no authority to obtain actions  $a_v$  of the victim agent and thus cannot utilize the true reward function defined by Equation (40). Instead, the adversary should define a surrogate extrinsic reward function inferred from the task. To reduce the bias introduced by manually designing a surrogate extrinsic reward, we use the following simple surrogate extrinsic reward

$$\hat{r}^{e1} = \omega_v v_x + 1, \quad (41)$$

where  $\omega_v$  is a constant coefficient to balance the forward reward and the living bonus 1.

*Evaluation Metrics.* We select vanilla PPO which uses Equation (9) as the objective and five robust training methods for the victim policy learning and report the average episodic rewards of these models under no attack and against various black-box attacks. Our selected robust training methods include (1) SA [73] improving the robustness of PPO via a smooth policy regularization (denoted as SA-regularizer for concision) on policy network solved by convex relaxations; (2) ATLA [72] alternately training the agent and an RL attacker with independent value and policy networks; (3) ATLA-SA [72] combining ATLA training framework and SA-regularizer and using LSTM as the policy network; (4) RADIAL [43] leveraging an adversarial loss function based on bounds of the policy network under bounded  $l_\infty$  attacks; (5) WocaR [32] directly estimating and optimizing the worse-case cumulative episode rewards based on bounds of the policy network under bounded  $l_\infty$  attacks. In sum, SA, RADIAL, and WocaR belong to certified robust regularizer-based defense methods against evasion attacks, while ATLA and ATLA-SA belong to adversarial training defense methods. We use the released robust models as the victim. WocaR is the state-of-the-art robust RL method.

### 6.1.2 Sparse-Reward Single-Agent Locomotion Tasks.

*Task Description.* In the six sparse-reward locomotion tasks, the victim agent starts from the initial position and needs to move forward across a distant line to complete the task and obtain an extrinsic reward signal. The episode is terminated once the victim agent gets the extrinsic reward or steps into unhealthy states defined by the task. The episode will be truncated when the length is larger than 500 timesteps. The sparse reward function is defined as

$$r^{e2} = \mathbb{1}[x \geq x_g] - b_2, \quad (42)$$

where  $\mathbb{1}[\cdot]$  is the indicator function, and  $b_2$  is a living cost to force the victim agent to move as fast as possible. Still, the adversary does not know the training procedure of the victim agent and should infer a surrogate extrinsic reward. Since  $r^{e2}$  is already sparse and easy to be inferred from the task description, we set the surrogate extrinsic reward the same as the true sparse reward, that is,  $\hat{r}^{e2} = r^{e2}$ .

*Evaluation Metrics.* We train the victim agent with an auxiliary objective and report average episode true rewards under various attacks. Since the extrinsic reward signal  $r^{e2}$  is sparse, vanilla PPO cannot directly solve these tasks. To successfully solve the task, we utilize  $J_{e1}^v(d^{\pi^v}) = \sum_s d^{\pi^v}(s) r^{e1}(s)$  as an auxiliary objective for the victim agent to encourage it to move forward in the early stage of training and gradually decay the strength of the regularizer to reduce the bias introduced by this auxiliary objective, that is,

$$\max_{d^{\pi^v}} J_{e2}^v(d^{\pi^v}) + \omega^{e1} J_{e1}^v(d^{\pi^v}). \quad (43)$$

where  $J_{e2}^v(d^{\pi^v}) = \sum_s d^{\pi^v}(s) r^{e2}(s)$  is the victim's original objective. In experiments, we found linearly or exponentially decaying  $\omega^{e1}$  result in low success rates and thus leverage the Lagrangian method similar to Equation (37) to adaptively update  $\omega^{e1}$  as following

$$\omega_k^{e1} = \omega_{k-1}^{e1} - \eta (J_{e2}^v(d^{\pi^v_k}) - \beta J_{e2}^v(d^{\pi^v_{k-1}})). \quad (44)$$

### 6.1.3 Sparse-Reward Single-Agent Navigation Task.

*Task Description.* To further validate the attack performance of our IMAP, we also select a sparse-reward single-agent navigation task named AntUMaze. The environment of AntUMaze is shown in Figure 3b. The Ant in the AntUMaze task is required to navigate in the U-shape maze to reach the target region instead of just running forward as fast as possible and thus more complex than Ant and SparseAnt tasks. The sparse reward function for this task is defined as

$$r^{e3} = \mathbb{1}[\|p - p_g\| \leq \epsilon] - b_3, \quad (45)$$

where  $p$  and  $p_g$  are the Ant position vector and the target vector separately,  $b_3$  is a constant cost to encourage the victim policy to search the shortest trajectory. Similar to sparse-reward locomotion tasks, the surrogate extrinsic reward for the adversary is set to  $\hat{r}^{e3} = r^{e3}$  for concision.

*Evaluation Metrics.* We train the victim agent for AntUMaze with data-based intrinsic motivation and report average episode true rewards under various attacks to avoid complex reward shaping. The objective of the victim agent is

$$\max_{d^{\pi^v}} J_{e3}^v(d^{\pi^v}) + \tau_k J_1^v(d^{\pi^v}) \quad (46)$$

where  $J_i^v(d^{\pi^v})$  is the intrinsic motivation encouraging the victim agent to explore the maze, and  $\tau_k$  is updated according to Equation (37) and Equation (39).

### 6.1.4 Sparse-Reward Multi-Agent Competition Tasks.

*Task Description.* For multi-agent competition tasks, we select two two-player zero-sum competition games YouShallNotPass and KickAndDefend, which have been widely adopted in previous adversarial policy research. The environment is visualized in Figure 3c and Figure 3d. In YouShallNotPass, two humanoid robots are initialized facing each other. The victim policy controls the runner (blue), and the adversarial policy controls the blocker (red). The runner wins if it reaches the finish line within 500 timesteps; the blocker wins if the runner does not win. KickAndDefend is a soccer penalty shootout between two humanoid robots. The victim policy controls the kicker (blue), and the adversarial policy controls the goalie (red). The kicker wins if it shoots the ball into the red gate within 500 timesteps; otherwise, the goalie wins. The sparse reward in these two tasks is defined as

$$r^{e4} = \mathcal{I}[\text{the victim wins}]. \quad (47)$$

Since these two games are zero-sum, the surrogate extrinsic reward for the adversary is the same as  $r^{e4}$ , that is,  $\hat{r}^{e4} = r^{e4}$ .

*Evaluation Metrics.* Note that instead of reporting the true average episode rewards of victim policies under various attacks, we report the success rates of different adversarial policies when playing with victim policies. The adversary’s success rate *ASR* is defined as

$$ASR = \frac{\text{the number of episodes where the adversary wins}}{\text{the number of total episodes}} \quad (48)$$

where the adversary’s latest policy collects the total episodes. The victim policies were trained via self-playing against random old versions of their opponents. As previous works did, we use the pre-trained victim policy weights released by [5].

## 6.2 Baselines and Implementation

We now introduce the baselines used in our experiments.

*6.2.1 Single-Agent Tasks.* We select SA-RL [72], the state-of-the-art black-box adversarial policy for single-agent evasion attack on state space, as the baseline. Since our threat model assumes that the adversary can not obtain the true reward used in the victim training, we use SA-RL-s to denote SA-RL with the surrogate victim reward function. Since the true and surrogate victim reward in sparse-reward is similar or the same, we don’t make distinctions between SA-RL and SA-RL-s in sparse-reward tasks. All attacking methods use the same attacking budget  $\epsilon$  in each task.

*6.2.2 Multi-Agent Tasks.* We choose AP-MARL [16], the state-of-the-art black-box adversarial policy for multi-agent tasks, as the baseline. Although several adversarial policy learning methods for multi-agent tasks have been developed after AP, they either need to train a surrogate victim policy [69] or value network [17], or target non-zero-sum games [18] or cooperative games [30]. In contrast, we don’t need to train any surrogate victim model and are interested in zero-sum competitive games.

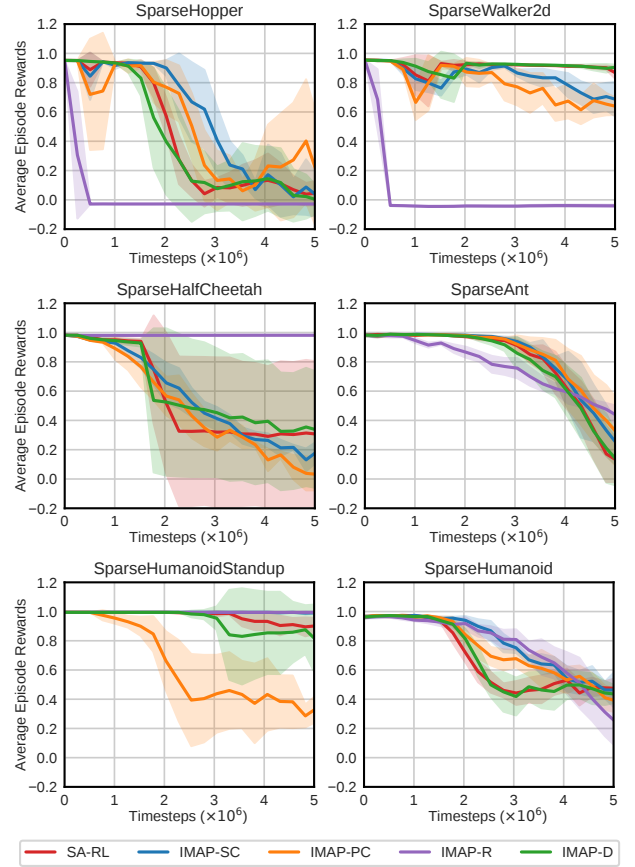


**Figure 4: Curve of test-time attacking results of SA-RL and four IMAP variants on six sparse-reward locomotion tasks.**

## 6.3 IMAP in Single-Agent Tasks

*6.3.1 Dense-Reward Locomotion Tasks.* ?? presents results of three baseline attacks (Random, SA-RL, SA-RL-s) and four IMAP variants (IMAP-SC, IMAP-PC, IMAP-R, IMAP-D) on attacking vanilla PPO and robustly trained ATLA, SA, ATLA-SA, RADIAL, and WocaR. IMAP-SC, IMAP-PC, IMAP-R, and IMAP-D use the state-coverage-driven, policy-coverage-driven, risk-driven, and divergence-driven intrinsic objectives separately. RADIAL and WocaR do not release their models for Ant, so we omit them. From ??, we can see that IMAP performs best against most models compared with other adversarial policies and show the best average performance. IMAP variants reduce 13 out of 22 models’ average episode rewards to the lowest, while SA-RL only 6. Among all IMAP variants, IMAP-PC shows the best average performance (bold in Avg. Rew. line), suggesting the advantage of coverage-driven intrinsic objectives compared with risk-driven and divergence-driven ones. The average performance of all models in Hopper, Walker, HalfCheetah, and Ant under IMAP-PC are reduced by 65.66%, 40.52%, 55.97%, and 69.94% separately. Notably, for the state-of-the-art WocaR robust models, our IMAP reduces the average episode rewards by a significant margin, that is, 54.58%, 34.07%, and 38.10% in Hopper,

**Table 1: Average episode rewards  $\pm$  standard deviation of six types of models, including PPO (vanilla), ATLA, SA, ATLA-SA, RADIAL, and WocaR, over 300 episodes under three baselines attacks, including Random, SA-RL, SA-RL-s (SA-RL with a surrogate victim reward) and four IMAP variants, including state-coverage-driven IMAP-SC, policy-coverage-driven IMAP-PC, risk-driven IMAP-R, and diversity-driven IMAP-D, on four dense-reward MuJoCo locomotion tasks, including Hopper, Walker2d, HalfCheetah, and Ant. Natural rewards of all models are also reported. To compare the overall performance, we also report the average reward of six types of models under the same attack on each environment. We bold the best attack result (the lowest value) under each row. IMAP-PC outperforms other black-box attacks on most models and shows the best average performance on each task.**

Env.	Model	Natural Reward	Random	SA-RL	SA-RL-s	IMAP-SC (ours)	IMAP-PC (ours)	IMAP-R (ours)	IMAP-D (ours)
Hop.	PPO (va.)	3167 $\pm$ 542	2101 $\pm$ 793	636 $\pm$ 9	<b>80 <math>\pm</math> 2</b>	<b>80 <math>\pm</math> 2</b>	<b>80 <math>\pm</math> 2</b>	<b>80 <math>\pm</math> 2</b>	<b>80 <math>\pm</math> 2</b>
	ATLA	2559 $\pm$ 958	2153 $\pm$ 882	976 $\pm$ 40	875 $\pm$ 145	689 $\pm$ 132	<b>639 <math>\pm</math> 48</b>	672 $\pm$ 120	808 $\pm$ 170
	SA	3705 $\pm$ 2	2710 $\pm$ 801	<b>1076 <math>\pm</math> 791</b>	1826 $\pm$ 897	1282 $\pm$ 68	1346 $\pm$ 85	1714 $\pm$ 1176	2278 $\pm$ 1144
	11D ATLA-SA	3291 $\pm$ 600	3165 $\pm$ 576	1772 $\pm$ 802	1585 $\pm$ 469	1685 $\pm$ 512	<b>1536 <math>\pm</math> 392</b>	1807 $\pm$ 642	1823 $\pm$ 527
	0.075 RADIAL	3740 $\pm$ 44	3729 $\pm$ 100	1722 $\pm$ 186	<b>1622 <math>\pm</math> 408</b>	2194 $\pm$ 672	1647 $\pm$ 398	1871 $\pm$ 498	1895 $\pm$ 551
	WocaR	3616 $\pm$ 99	3633 $\pm$ 30	2390 $\pm$ 145	1850 $\pm$ 530	2140 $\pm$ 612	<b>1646 <math>\pm</math> 337</b>	2917 $\pm$ 495	1832 $\pm$ 493
	Avg. Rew.	3346	2915	1429	1306	1345	<b>1149</b>	1510	1452
Wal.	PPO (va.)	4472 $\pm$ 635	3007 $\pm$ 1200	1086 $\pm$ 516	1253 $\pm$ 468	1002 $\pm$ 391	<b>895 <math>\pm</math> 450</b>	2966 $\pm$ 956	947 $\pm$ 160
	ATLA	3138 $\pm$ 1061	3384 $\pm$ 1056	2213 $\pm$ 915	1163 $\pm$ 464	1035 $\pm$ 614	<b>991 <math>\pm</math> 500</b>	1599 $\pm$ 742	1385 $\pm$ 590
	SA	4487 $\pm$ 61	4465 $\pm$ 39	<b>2908 <math>\pm</math> 336</b>	3927 $\pm$ 162	4196 $\pm$ 231	3072 $\pm$ 1304	4083 $\pm$ 155	3820 $\pm$ 39
	17D ATLA-SA	3842 $\pm$ 475	3927 $\pm$ 368	3663 $\pm$ 707	3508 $\pm$ 66	3144 $\pm$ 995	<b>2868 <math>\pm</math> 1145</b>	3620 $\pm$ 143	3469 $\pm$ 650
	0.05 RADIAL	5251 $\pm$ 12	5184 $\pm$ 42	<b>3320 <math>\pm</math> 245</b>	4376 $\pm$ 1229	4562 $\pm$ 941	4377 $\pm$ 1147	4584 $\pm$ 1021	4474 $\pm$ 1187
	WocaR	4156 $\pm$ 495	4244 $\pm$ 157	3770 $\pm$ 196	2871 $\pm$ 1153	3178 $\pm$ 1168	2874 $\pm$ 1085	<b>2740 <math>\pm</math> 1162</b>	2859 $\pm$ 1078
	Avg. Rew.	4224	4035	2827	2850	2853	<b>2513</b>	3265	2826
Half.	PPO (va.)	7117 $\pm$ 98	5486 $\pm$ 1378	<b>0 <math>\pm</math> 0</b>	<b>0 <math>\pm</math> 0</b>	<b>0 <math>\pm</math> 0</b>	<b>0 <math>\pm</math> 0</b>	56 $\pm$ 147	<b>0 <math>\pm</math> 0</b>
	ATLA	5417 $\pm$ 49	5388 $\pm$ 34	2709 $\pm$ 80	<b>1696 <math>\pm</math> 1352</b>	2451 $\pm$ 1352	1711 $\pm$ 1357	1996 $\pm$ 965	1765 $\pm$ 1357
	SA	3632 $\pm$ 20	3619 $\pm$ 18	3028 $\pm$ 23	2997 $\pm$ 22	2996 $\pm$ 24	<b>2984 <math>\pm</math> 20</b>	3390 $\pm$ 62	3000 $\pm$ 27
	17D ATLA-SA	6157 $\pm$ 852	6164 $\pm$ 603	5058 $\pm$ 418	<b>4170 <math>\pm</math> 664</b>	4311 $\pm$ 412	4202 $\pm$ 726	4395 $\pm$ 728	4231 $\pm$ 681
	0.15 RADIAL	4724 $\pm$ 14	4731 $\pm$ 42	3253 $\pm$ 131	1654 $\pm$ 1312	1669 $\pm$ 1326	<b>1641 <math>\pm</math> 1298</b>	1791 $\pm$ 1278	2563 $\pm$ 1496
	WocaR	6032 $\pm$ 68	5969 $\pm$ 149	5365 $\pm$ 54	4257 $\pm$ 1254	<b>3734 <math>\pm</math> 1512</b>	4026 $\pm$ 1374	4782 $\pm$ 105	4759 $\pm$ 487
	Avg. Rew.	5513	5226	3236	2462	2433	<b>2427</b>	2730	
Ant	PPO (va.)	5687 $\pm$ 758	5261 $\pm$ 1005	<b>0 <math>\pm</math> 0</b>	351 $\pm$ 110	310 $\pm$ 184	212 $\pm$ 244	188 $\pm$ 135	284 $\pm$ 195
	ATLA	4894 $\pm$ 123	4541 $\pm$ 691	33 $\pm$ 327	<b>0 <math>\pm</math> 0</b>	428 $\pm$ 63	70 $\pm$ 128	696 $\pm$ 24	<b>0 <math>\pm</math> 0</b>
	111D SA	4292 $\pm$ 384	4986 $\pm$ 452	<b>2511 <math>\pm</math> 1117</b>	2698 $\pm$ 822	2720 $\pm$ 879	2643 $\pm$ 851	2722 $\pm$ 994	2746 $\pm$ 831
	0.15 ATLA-SA	5359 $\pm$ 153	5366 $\pm$ 104	3765 $\pm$ 101	3125 $\pm$ 207	3228 $\pm$ 190	3156 $\pm$ 302	<b>2611 <math>\pm</math> 213</b>	3125 $\pm$ 182
	Avg. Rew.	5058	5039	1577	1544	1672	<b>1520</b>	1554	1539

Walker, and HalfCheetah respectively. Surprisingly, in Walker2d and HalfCheetah, although the WocaR model is the most robust model under SA-RL, the performance can still be decreased by our IMAP variants and is worse than RADIAL and ATLA-SA. This denotes that a weak adversarial policy may give a false sense of robustness. Moreover, IMAP-SC, IMAP-PC, and IMAP-R achieve the best performance when attacking WocaR in HalfCheetah, Hopper, and Walker2d separately, suggesting that we should try multiple types of intrinsic objectives when attacking robust RL models.

Comparing SA-RL and SA-RL-s in ??, we can see the advantage of utilizing the simple surrogate victim reward  $f^{e1}$ . SA-RL-s performs better than SA-RL when attacking 16 out of 22 models. Especially, SA-RL-s dominates SA-RL in HalfCheetah. Intuitively, the true victim reward includes various items like control input and contact force costs, which might be unstable and obfuscate the adversary to find a suboptimal attack strategy.

For the two coverage-driven intrinsic objectives, IMAP-PC performs better than IMAP-SC, suggesting that the adversary should be aware of past state distributions instead of only current state distributions in these dense-reward locomotion tasks. Intuitively, although IMAP-SC encourages the adversary to lure the victim into covering states uniformly, it might vary near the optimal trajectory; IMAP-PC instead stimulates the adversary to lure the victim into deviating from all past optimal trajectories by maximizing the entropy of the policy coverage.

In experiments, we found that the bias reduction method BR does not boost much performance of IMAP variants in dense-reward locomotion tasks, so we ignore the results of IMAP variants+BR in Table 1. This might be caused by the difficulty of approximating

**Table 2: Average episode rewards  $\pm$  standard deviation of six locomotion victim agents in SparseHopper, SparseWalker, SparseHalfCheetah, SparseWalker, SparseAnt, SparseHumanoidStandup, and SparseHumanoid, and two navigation agents in AntUMaze and Ant4Rooms under nine attacks including SA, four IMAP variants and four IMAP variants with the BR method. We bold the best attack result (the lowest value) under each row and underline the results that BR improves IMAP variants. The natural rewards of all victim agents are near one, so we do not include them in the table. IMAP performs better than SA-RL in all tasks, and BR can further improve the performance of IMAP in half of the tasks.**

Env.	SA-RL	IMAP-SC	IMAP-PC	IMAP-R	IMAP-D	IMAP-SC + BR	IMAP-PC + BR	IMAP-R + BR	IMAP-D + BR
S.Hop.	0.01 $\pm$ 0.32	0.00 $\pm$ 0.30	0.16 $\pm$ 0.45	-0.03 $\pm$ 0.00	-0.02 $\pm$ 0.28	<u>-0.01 <math>\pm</math> 0.28</u>	<b><u>-0.05 <math>\pm</math> 0.22</u></b>	-0.02 $\pm$ 0.27	0.01 $\pm$ 0.32
S.Wal.	0.85 $\pm$ 0.23	0.66 $\pm$ 0.44	0.63 $\pm$ 0.45	<b>-0.04 <math>\pm</math> 0.01</b>	0.91 $\pm$ 0.06	0.91 $\pm$ 0.06	0.84 $\pm$ 0.26	0.80 $\pm$ 0.32	<u>0.90 <math>\pm</math> 0.12</u>
S.Half.	0.30 $\pm$ 0.51	0.17 $\pm$ 0.45	<b>0.04 <math>\pm</math> 0.35</b>	0.98 $\pm$ 0.00	0.33 $\pm$ 0.51	<u>0.06 <math>\pm</math> 0.37</u>	0.07 $\pm$ 0.38	0.98 $\pm$ 0.00	<u>0.12 <math>\pm</math> 0.43</u>
S.Ant.	0.12 $\pm$ 0.42	0.23 $\pm$ 0.48	0.27 $\pm$ 0.49	0.43 $\pm$ 0.49	0.12 $\pm$ 0.42	<u>0.11 <math>\pm</math> 0.42</u>	<u>0.13 <math>\pm</math> 0.43</u>	0.96 $\pm$ 0.10	<b><u>0.10 <math>\pm</math> 0.40</u></b>
S.Hu.St.	0.88 $\pm$ 0.32	0.99 $\pm$ 0.05	<b>0.23 <math>\pm</math> 0.50</b>	0.99 $\pm$ 0.00	0.80 $\pm$ 0.42	0.99 $\pm$ 0.05	0.36 $\pm$ 0.54	0.99 $\pm$ 0.00	0.87 $\pm$ 0.35
S.Hu.	0.49 $\pm$ 0.50	0.46 $\pm$ 0.50	0.40 $\pm$ 0.49	<b>0.24 <math>\pm</math> 0.44</b>	0.45 $\pm$ 0.5	0.47 $\pm$ 0.50	<u>0.35 <math>\pm</math> 0.48</u>	0.43 $\pm$ 0.5	0.53 $\pm$ 0.49
A.UM.	0.32 $\pm$ 0.52	0.30 $\pm$ 0.51	0.37 $\pm$ 0.52	0.97 $\pm$ 0.10	0.28 $\pm$ 0.51	0.36 $\pm$ 0.52	<b><u>0.19 <math>\pm</math> 0.47</u></b>	0.97 $\pm$ 0.07	0.34 $\pm$ 0.52
A.4R.	0.34 $\pm$ 0.51	0.32 $\pm$ 0.51	0.40 $\pm$ 0.52	0.74 $\pm$ 0.43	0.24 $\pm$ 0.48	0.43 $\pm$ 0.52	<u>0.33 <math>\pm</math> 0.51</u>	<b><u>0.22 <math>\pm</math> 0.48</u></b>	0.24 $\pm$ 0.49

$\max_d J_e^a(d)$  in dense-reward tasks. However, we observe significant improvement brought about by BR in sparse-reward single-agent and multi-agent tasks. We will discuss the effect of BR in Section 6.3.2 and Section 6.4.

**6.3.2 Sparse-Reward Locomotion and Navigation Tasks.** Figure 4 shows the results of the baseline SA-RL and four IMAP variants in six sparse-reward locomotion tasks. From Figure 4, we can see that intrinsic objectives help improve the performance of the adversarial policy. IMAP-R performs best in SparseHopper and SparseWalker2d and learns  $5 \times 10^6$  faster than others. This demonstrates that agents that are 'robust' to one type of adversarial policy may be vulnerable to another type of intrinsically motivated adversarial policy. We can also see that IMAP-PC performs best in SparseHumanoidStandup, while IMAP-R performs even worse than SA-RL, denoting that the Humanoid is robust to the risk-driven intrinsic objective but is still fragile to PC-driven intrinsic objective. In other tasks like SparseHalfCheetah and SparseHumanoid, IMAP variants also improve the performance of SA-RL by a large margin. What's more, IMAP performs better than SA-RL in navigation tasks AntUMaze and Ant4Rooms, as shown in Table 2. Specifically, when BR is not applied, IMAP-D achieves the best results, demonstrating the effectiveness of the divergence-driven intrinsic objective.

**Ablation on Bias-Reduction.** To investigate the effectiveness of BR, we report the results of IMAP variants with BR in Table 2. BR can further improve the performance of IMAP in half of 8 sparse-reward tasks by reducing the bias introduced by the intrinsic objective. For instance, a clear distraction phenomenon exists in IMAP-PC in SparseHopper, as shown in Figure 4. By applying BR to IMAP-PC, the average episode rewards can be reduced from 0.16 to -0.05. We underline the results where BR takes a positive effect. Note that BR cannot always help improve the performance of IMAP variants, especially when the task is challenging, like SparseWalker2d or SparseHumanoidStandup. This is reasonable since, in these challenging tasks, the extrinsic reward might provide a wrong optimization direction. For instance, in SparseWalker2d, SA-RL tries to make the episode as long as possible to increase the cumulative

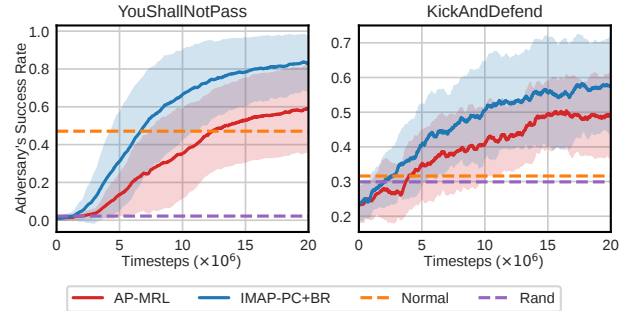


**Figure 5: Learning curve of AP-MRL and IAMP in two two-player zero-sum games. IMAP improves the adversary's success rate by a large margin.**

cost  $\sum -b_2$ . However, this strategy is ineffective in reducing the cumulative reward signal  $\sum \mathbb{1}[x \geq x_g]$ . Thus, when the strength of intrinsic motivation decrease, the adversary might be trapped again in this kind of local optima and cannot escape anymore.

## 6.4 IMAP in multi-agent tasks

Figure 5 shows the results of IMAP in multi-agent tasks. IMAP-PC+BR performs best than other IMAP variants. IMAP-PC improves ASR from AP-MRL's 59.64% to 83.91% by learning a more natural attacking behavior in YouShallNotPass as shown in Figure 2 without knowledge of the victim. This demonstrates the effectiveness of maximum PC entropy as designed in Equation (20). In KickAndDefend, the goalie is restricted in a square region before the gate according to the game rule, and thus the adversary cannot control the goalie to 'aggressively' attack the victim kicker. Even with such restriction, IMAP still improves ASR from 47.02% to 56.96% in KickAndDefend, again showing intrinsic motivation's benefit in searching the optimal adversarial policy.

## 7 CONCLUSION

In this paper, we proposed Intrinsically Motivated Adversarial Policy (IMAP) to launch test-time black-box evasion attacks against RL agents in single- and multi-agent environments. We developed four IMAP variants, namely, IMAP-SC, IMAP-PC, IMAP-R, and IMAP-D, based on state-coverage-driven, policy-coverage-driven, risk-driven, and divergence-driven intrinsic objectives separately. We evaluated the effectiveness of IMAP variants in various MuJoCo environments. The results showed that our IMAP learned stronger adversarial policies. To reduce the bias introduced by the intrinsic objective, we also developed a bias-reduction method BR and empirically showed that BR can effectively boost the performance of IMAP in sparse-reward tasks. We found that IMAP could defeat the state-of-the-art robust RL agents, proposing a new challenge to defend the RL agents against IMAP.

## REFERENCES

- [1] Brendon G Anderson and Somayeh Sojoudi. 2022. Certified robustness via locally biased randomized smoothing. In *Learning for Dynamics and Control Conference*. PMLR, 207–220.
- [2] Szilárd Aradi. 2020. Survey of deep reinforcement learning for motion planning of autonomous vehicles. *IEEE Transactions on Intelligent Transportation Systems* 23, 2 (2020), 740–759.
- [3] Chenjia Bai, Lingxiao Wang, Lei Han, Jianye Hao, Animesh Garg, Peng Liu, and Zhaoran Wang. 2021. Principled exploration via optimistic bootstrapping and backward induction. In *International Conference on Machine Learning*. PMLR, 577–587.
- [4] Xiaoxuan Bai, Wenjia Niu, Jiqiang Liu, Xu Gao, Yingxiao Xiang, and Jingjing Liu. 2018. Adversarial examples construction towards white-box Q table variation in DQN pathfinding training. In *2018 IEEE Third International Conference on Data Science in Cyberspace (DSC)*. IEEE, 781–787.
- [5] Trapit Bansal, Jakub Pachocki, Szymon Sidor, Ilya Sutskever, and Igor Mor-datch. 2017. Emergent complexity via multi-agent competition. *arXiv preprint arXiv:1710.03748* (2017).
- [6] Vahid Behzadan and Arslan Munir. 2017. Whatever does not kill deep reinforcement learning, makes it stronger. *arXiv preprint arXiv:1712.09344* (2017).
- [7] Vahid Behzadan and Arslan Munir. 2018. Mitigation of policy manipulation attacks on deep q-networks with parameter-space noise. In *Computer Safety, Reliability, and Security: SAFECOMP 2018 Workshops, ASSURE, DECSos, SASSUR, STRIVE, and WAISE, Västerås, Sweden, September 18, 2018, Proceedings 37*. Springer International Publishing, 406–417.
- [8] Marc Bellemare, Sriram Srinivasan, Georg Ostrovski, Tom Schaul, David Saxton, and Remi Munos. 2016. Unifying count-based exploration and intrinsic motivation. *Advances in neural information processing systems* 29 (2016).
- [9] Prasanth Buddareddygar, Travis Zhang, Yezhou Yang, and Yi Ren. 2022. Targeted Attack on Deep RL-based Autonomous Driving with Learned Visual Patterns. In *2022 International Conference on Robotics and Automation (ICRA)*. IEEE, 10571–10577.
- [10] Yuri Burda, Harrison Edwards, Amos Storkey, and Oleg Klimov. 2018. Exploration by random network distillation. *arXiv preprint arXiv:1810.12894* (2018).
- [11] Tong Chen, Wenjia Niu, Yingxiao Xiang, Xiaoxuan Bai, Jiqiang Liu, Zhen Han, and Gang Li. 2018. Gradient band-based adversarial training for generalized attack immunity of A3C path finding. *arXiv preprint arXiv:1807.06752* (2018).
- [12] Andre Esteva, Alexandre Robicquet, Bharath Ramsundar, Volodymyr Kuleshov, Mark DePristo, Katherine Chou, Claire Cui, Greg Corrado, Sebastian Thrun, and Jeff Dean. 2019. A guide to deep learning in healthcare. *Nature medicine* 25, 1 (2019), 24–29.
- [13] Michael Everett. 2021. Neural network verification in control. In *2021 60th IEEE Conference on Decision and Control (CDC)*. IEEE, 6326–6340.
- [14] Justin Fu, John Co-Reyes, and Sergey Levine. 2017. Ex2: Exploration with exemplar models for deep reinforcement learning. *Advances in neural information processing systems* 30 (2017).
- [15] Ted Fujimoto, Timothy Doster, Adam Attarian, Jill Brandenberger, and Nathan Hodas. 2021. Reward-free attacks in multi-agent reinforcement learning. *arXiv preprint arXiv:2112.00940* (2021).
- [16] Adam Gleave, Michael Dennis, Cody Wild, Neel Kant, Sergey Levine, and Stuart Russell. 2019. Adversarial policies: Attacking deep reinforcement learning. *arXiv preprint arXiv:1905.10615* (2019).
- [17] Chen Gong, Zhou Yang, Yunpeng Bai, Jieke Shi, Arunesh Sinha, Bowen Xu, David Lo, Xinwen Hou, and Guoliang Fan. 2022. Curiosity-driven and victim-aware adversarial policies. In *Proceedings of the 38th Annual Computer Security Applications Conference*. 186–200.
- [18] Wenbo Guo, Xian Wu, Sui Huang, and Xinyu Xing. 2021. Adversarial policy learning in two-player competitive games. In *International Conference on Machine Learning*. PMLR, 3910–3919.
- [19] Wenbo Guo, Xian Wu, Usmann Khan, and Xinyu Xing. 2021. Edge: Explaining deep reinforcement learning policies. *Advances in Neural Information Processing Systems* 34 (2021), 12222–12236.
- [20] Elad Hazan, Sham Kakade, Karan Singh, and Abby Van Soest. 2019. Provably efficient maximum entropy exploration. In *International Conference on Machine Learning*. PMLR, 2681–2691.
- [21] Jiafan He, Dongruo Zhou, and Quanquan Gu. 2021. Nearly minimax optimal reinforcement learning for discounted MDPs. *Advances in Neural Information Processing Systems* 34 (2021), 22288–22300.
- [22] Yonghong Huang and Shih-han Wang. 2018. Adversarial manipulation of reinforcement learning policies in autonomous agents. In *2018 International Joint Conference on Neural Networks (IJCNN)*. IEEE, 1–8.
- [23] Chi Jin, Zhuoran Yang, Zhaoran Wang, and Michael I Jordan. 2020. Provably efficient reinforcement learning with linear function approximation. In *Conference on Learning Theory*. PMLR, 2137–2143.
- [24] B Ravi Kiran, Ibrahim Sobh, Victor Talpaert, Patrick Mannion, Ahmad A Al Sallab, Senthil Yogamani, and Patrick Pérez. 2021. Deep reinforcement learning for autonomous driving: A survey. *IEEE Transactions on Intelligent Transportation Systems* 23, 6 (2021), 4909–4926.
- [25] Ezgi Korkmaz. 2021. Investigating vulnerabilities of deep neural policies. In *Uncertainty in Artificial Intelligence*. PMLR, 1661–1670.
- [26] Aounon Kumar, Alexander Levine, and Soheil Feizi. 2021. Policy smoothing for provably robust reinforcement learning. *arXiv preprint arXiv:2106.11420* (2021).
- [27] Michael Laskin, Denis Yarats, Hao Liu, Kimin Lee, Albert Zhan, Kevin Lu, Catherine Cang, Lerrel Pinto, and Pieter Abbeel. 2021. URLB: Unsupervised reinforcement learning benchmark. *arXiv preprint arXiv:2110.15191* (2021).
- [28] Kimin Lee, Michael Laskin, Aravind Srinivas, and Pieter Abbeel. 2021. Sunrise: A simple unified framework for ensemble learning in deep reinforcement learning. In *International Conference on Machine Learning*. PMLR, 6131–6141.
- [29] Xian Yeow Lee, Sambit Ghadai, Kai Liang Tan, Chinmay Hegde, and Soumik Sarkar. 2020. Spatiotemporally constrained action space attacks on deep reinforcement learning agents. In *Proceedings of the AAAI conference on artificial intelligence*, Vol. 34. 4577–4584.
- [30] Simin Li, Jun Guo, Jingqiao Xiu, Pu Feng, Xin Yu, Jiakai Wang, Aishan Liu, Wenjun Wu, and Xianglong Liu. 2023. Attacking Cooperative Multi-Agent Reinforcement Learning by Adversarial Minority Influence. *arXiv preprint arXiv:2302.03322* (2023).
- [31] Yinkang Li, Xiaolong Hao, Yuchen She, Shuang Li, and Meng Yu. 2021. Constrained motion planning of free-float dual-arm space manipulator via deep reinforcement learning. *Aerospace Science and Technology* 109 (2021), 106446.
- [32] Yongyuan Liang, Yanchao Sun, Ruijie Zheng, and Furong Huang. 2022. Efficient Adversarial Training without Attacking: Worst-Case-Aware Robust Reinforcement Learning. *arXiv preprint arXiv:2210.05927* (2022).
- [33] Yen-Chen Lin, Zhang-Wei Hong, Yuan-Hong Liao, Meng-Li Shih, Ming-Yu Liu, and Min Sun. 2017. Tactics of adversarial attack on deep reinforcement learning agents. *arXiv preprint arXiv:1703.06748* (2017).
- [34] Yen-Chen Lin, Ming-Yu Liu, Min Sun, and Jia-Bin Huang. 2017. Detecting adversarial attacks on neural network policies with visual foresight. *arXiv preprint arXiv:1710.00814* (2017).
- [35] Hao Liu and Pieter Abbeel. 2021. Aps: Active pretraining with successor features. In *International Conference on Machine Learning*. PMLR, 6736–6747.
- [36] Hao Liu and Pieter Abbeel. 2021. Behavior from the void: Unsupervised active pre-training. *Advances in Neural Information Processing Systems* 34 (2021), 18459–18473.
- [37] Björn Lütjens, Michael Everett, and Jonathan P How. 2020. Certified adversarial robustness for deep reinforcement learning. In *Conference on Robot Learning*. PMLR, 1328–1337.
- [38] Michael Lutter, Shie Mannor, Jan Peters, Dieter Fox, and Animesh Garg. 2021. Robust value iteration for continuous control tasks. *arXiv preprint arXiv:2105.12189* (2021).
- [39] Aleksander Madry, Aleksandar Makelov, Ludwig Schmidt, Dimitris Tsipras, and Adrian Vladu. 2017. Towards deep learning models resistant to adversarial attacks. *arXiv preprint arXiv:1706.06083* (2017).
- [40] Kanghua Mo, Weixuan Tang, Jin Li, and Xu Yuan. 2022. Attacking deep reinforcement learning with decoupled adversarial policy. *IEEE Transactions on Dependable and Secure Computing* (2022).
- [41] Mirco Mutti, Lorenzo Pratissoli, and Marcello Restelli. 2021. Task-agnostic exploration via policy gradient of a non-parametric state entropy estimate. In *Proceedings of the AAAI Conference on Artificial Intelligence*, Vol. 35. 9028–9036.
- [42] Gergely Neu and Julia Olshovskaya. 2021. Online learning in MDPs with linear function approximation and bandit feedback. *Advances in Neural Information Processing Systems* 34 (2021), 10407–10417.
- [43] Tuomas Oikarinen, Wang Zhang, Alexandre Megretski, Luca Daniel, and Tsui-Wei Weng. 2021. Robust deep reinforcement learning through adversarial loss.

- Advances in Neural Information Processing Systems* 34 (2021), 26156–26167.
- [44] Ian Osband, Daniel Russo, and Benjamin Van Roy. 2013. (More) efficient reinforcement learning via posterior sampling. *Advances in Neural Information Processing Systems* 26 (2013).
- [45] Ian Osband and Benjamin Van Roy. 2017. Why is posterior sampling better than optimism for reinforcement learning?. In *International conference on machine learning*. PMLR, 2701–2710.
- [46] Matteo Papini, Andrea Tirinzoni, Aldo Pacchiano, Marcello Restelli, Alessandro Lazaric, and Matteo Pirootta. 2021. Reinforcement learning in linear mdps: Constant regret and representation selection. *Advances in Neural Information Processing Systems* 34 (2021), 16371–16383.
- [47] Deepak Pathak, Pulkit Agrawal, Alexei A Efros, and Trevor Darrell. 2017. Curiosity-driven exploration by self-supervised prediction. In *International conference on machine learning*. PMLR, 2778–2787.
- [48] Deepak Pathak, Dhiraj Gandhi, and Abhinav Gupta. 2019. Self-supervised exploration via disagreement. In *International conference on machine learning*. PMLR, 5062–5071.
- [49] Anay Pattanaik, Zhenyi Tang, Shuijing Liu, Gautham Bommanan, and Girish Chowdhary. 2017. Robust deep reinforcement learning with adversarial attacks. *arXiv preprint arXiv:1712.03632* (2017).
- [50] Lerrel Pinto, James Davidson, Rahul Sukthankar, and Abhinav Gupta. 2017. Robust adversarial reinforcement learning. In *International Conference on Machine Learning*. PMLR, 2817–2826.
- [51] Ao Qu, Yihong Tang, and Wei Ma. 2021. Attacking deep reinforcement learning-based traffic signal control systems with colluding vehicles. *arXiv preprint arXiv:2111.02845* (2021).
- [52] John Schulman, Sergey Levine, Pieter Abbeel, Michael Jordan, and Philipp Moritz. 2015. Trust region policy optimization. In *International conference on machine learning*. PMLR, 1889–1897.
- [53] John Schulman, Philipp Moritz, Sergey Levine, Michael Jordan, and Pieter Abbeel. 2015. High-dimensional continuous control using generalized advantage estimation. *arXiv preprint arXiv:1506.02438* (2015).
- [54] John Schulman, Filip Wolski, Prafulla Dhariwal, Alec Radford, and Oleg Klimov. 2017. Proximal policy optimization algorithms. *arXiv preprint arXiv:1707.06347* (2017).
- [55] Aizaz Sharif and Dusica Marijan. 2021. Adversarial Deep Reinforcement Learning for Trustworthy Autonomous Driving Policies. *arXiv preprint arXiv:2112.11937* (2021).
- [56] Archit Sharma, Shixiang Gu, Sergey Levine, Vikash Kumar, and Karol Hausman. 2019. Dynamics-aware unsupervised discovery of skills. *arXiv preprint arXiv:1907.01657* (2019).
- [57] Qianli Shen, Yan Li, Haoming Jiang, Zhaoran Wang, and Tuo Zhao. 2020. Deep reinforcement learning with robust and smooth policy. In *International Conference on Machine Learning*. PMLR, 8707–8718.
- [58] Jianwen Sun, Tianwei Zhang, Xiaofei Xie, Lei Ma, Yan Zheng, Kangjie Chen, and Yang Liu. 2020. Stealthy and efficient adversarial attacks against deep reinforcement learning. In *Proceedings of the AAAI Conference on Artificial Intelligence*, Vol. 34. 5883–5891.
- [59] Yanchao Sun, Ruijie Zheng, Yongyuan Liang, and Furong Huang. 2021. Who is the strongest enemy? towards optimal and efficient evasion attacks in deep rl. *arXiv preprint arXiv:2106.05087* (2021).
- [60] Kai Liang Tan, Yasaman Esfandiari, Xian Yeow Lee, Soumik Sarkar, et al. 2020. Robustifying reinforcement learning agents via action space adversarial training. In *2020 American control conference (ACC)*. IEEE, 3959–3964.
- [61] Chen Tessler, Yonathan Efroni, and Shie Mannor. 2019. Action robust reinforcement learning and applications in continuous control. In *International Conference on Machine Learning*. PMLR, 6215–6224.
- [62] Eugene Vinitsky, Yuqing Du, Kanaad Parvate, Kathy Jang, Pieter Abbeel, and Alexandre Bayen. 2020. Robust reinforcement learning using adversarial populations. *arXiv preprint arXiv:2008.01825* (2020).
- [63] Shengjie Wang, Xiang Zheng, Yuxue Cao, and Tao Zhang. 2021. A multi-target trajectory planning of a 6-DoF free-floating space robot via reinforcement learning. In *2021 IEEE/RSJ International Conference on Intelligent Robots and Systems (IROS)*. IEEE, 3724–3730.
- [64] Tianhao Wang, Dongruo Zhou, and Quanquan Gu. 2021. Provably efficient reinforcement learning with linear function approximation under adaptivity constraints. *Advances in Neural Information Processing Systems* 34 (2021), 13524–13536.
- [65] Tony Tong Wang, Adam Gleave, Nora Belrose, Tom Tseng, Joseph Miller, Michael D Dennis, Yawen Duan, Viktor Pogrebnik, Sergey Levine, and Stuart Russell. 2022. Adversarial Policies Beat Professional-Level Go AIs. *arXiv preprint arXiv:2211.00241* (2022).
- [66] Tsui-Wei Weng, Krishnamurthy Dj Dvijotham, Jonathan Uesato, Kai Xiao, Sven Gowal, Robert Stanforth, and Pushmeet Kohli. 2020. Toward evaluating robustness of deep reinforcement learning with continuous control. In *International Conference on Learning Representations*.
- [67] Fan Wu, Linyi Li, Zijian Huang, Yevgeniy Vorobeychik, Ding Zhao, and Bo Li. 2021. Crop: Certifying robust policies for reinforcement learning through functional smoothing. *arXiv preprint arXiv:2106.09292* (2021).
- [68] Junlin Wu and Yevgeniy Vorobeychik. 2022. Robust Deep Reinforcement Learning through Bootstrapped Opportunistic Curriculum. In *International Conference on Machine Learning*. PMLR, 24177–24211.
- [69] Xian Wu, Wenbo Guo, Hua Wei, and Xinyu Xing. 2021. Adversarial Policy Training against Deep Reinforcement Learning. In *USENIX Security Symposium*. 1883–1900.
- [70] Chao Yu, Jiming Liu, Shamim Nemati, and Guosheng Yin. 2021. Reinforcement learning in healthcare: A survey. *ACM Computing Surveys (CSUR)* 55, 1 (2021), 1–36.
- [71] Mengran Yu and Shiliang Sun. 2022. Natural Black-Box Adversarial Examples against Deep Reinforcement Learning. In *Proceedings of the AAAI Conference on Artificial Intelligence*, Vol. 36. 8936–8944.
- [72] Huan Zhang, Hongge Chen, Duane Boning, and Cho-Jui Hsieh. 2021. Robust reinforcement learning on state observations with learned optimal adversary. *arXiv preprint arXiv:2101.08452* (2021).
- [73] Huan Zhang, Hongge Chen, Chaowei Xiao, Bo Li, Mingyan Liu, Duane Boning, and Cho-Jui Hsieh. 2020. Robust deep reinforcement learning against adversarial perturbations on state observations. *Advances in Neural Information Processing Systems* 33 (2020), 21024–21037.
- [74] Tianjun Zhang, Paria Rashidinejad, Jiantao Jiao, Yuandong Tian, Joseph E Gonzalez, and Stuart Russell. 2021. Made: Exploration via maximizing deviation from explored regions. *Advances in Neural Information Processing Systems* 34 (2021), 9663–9680.
- [75] Tianjun Zhang, Huazhe Xu, Xiaolong Wang, Yi Wu, Kurt Keutzer, Joseph E Gonzalez, and Yuandong Tian. 2021. Noveld: A simple yet effective exploration criterion. *Advances in Neural Information Processing Systems* 34 (2021), 25217–25230.
- [76] Zihan Zhang, Yuan Zhou, and Xiangyang Ji. 2021. Model-free reinforcement learning: from clipped pseudo-regret to sample complexity. In *International Conference on Machine Learning*. PMLR, 12653–12662.
- [77] Xiang Zheng, Xingjun Ma, and Cong Wang. 2022. CIM: Constrained Intrinsic Motivation for Sparse-Reward Continuous Control. *arXiv preprint arXiv:2211.15205* (2022).

Received 20 February 2007; revised 12 March 2009; accepted 5 June 2009